

1 Genetic, biochemical, and molecular characterization of *Methanosarcina barkeri*
2 mutants lacking three distinct classes of hydrogenase

3

4

5 Thomas D. Mand,^a Gargi Kulkarni,^{a*} William W. Metcalf^{a#}

6

7 ^aDepartment of Microbiology, University of Illinois at Urbana-Champaign, Urbana,
8 Illinois, USA

9

10 Running Head: Analysis of *M. barkeri* hydrogenase mutants

11

12 #Address correspondence to William W. Metcalf, metcalf@life.illinois.edu.

13 *Present address: Gargi Kulkarni, California Institute of Technology, Pasadena,
14 California, USA

15 T.D.M. and G.K. contributed equally to this work.

16

17 **ABSTRACT**

18 The methanogenic archaeon *Methanosarcina barkeri* encodes three distinct
19 types of hydrogenase, whose functions vary depending on the growth substrate.
20 These include the F420-dependent (Frh), methanophenazine-dependent (Vht), and
21 ferredoxin-dependent (Ech) hydrogenases. To investigate their physiological roles,
22 we characterized a series of mutants lacking each hydrogenase in various
23 combinations. Mutants lacking Frh, Vht, or Ech in any combination failed to grow on
24 H₂/CO₂, whereas only Vht and Ech were essential for growth on acetate. In contrast,
25 a mutant lacking all three grew on methanol with a final growth yield similar to
26 wild-type, produced methane and CO₂ in the expected 3:1 ratio, but had a *ca.* 33%
27 slower growth rate. Thus, hydrogenases play a significant, but non-essential, role
28 during growth on this substrate. As previously observed, mutants lacking Ech fail to
29 grow on methanol/H₂ unless supplemented with biosynthetic precursors.
30 Interestingly, this phenotype was abolished in the $\Delta ech/\Delta frh$ and $\Delta ech/\Delta frh/\Delta vht$
31 mutants, consistent with the idea that hydrogenases inhibit methanol oxidation in
32 the presence of H₂, which prevents production of reducing equivalents needed for
33 biosynthesis. Quantification of methane and CO₂ produced from methanol by
34 resting cell suspensions of various mutants supports this conclusion. Based on
35 global transcriptional profiles, none of the hydrogenases are upregulated to
36 compensate for loss of the others. However, transcript levels of the F420
37 dehydrogenase operon were significantly higher in all strains lacking *frh*, suggesting
38 a mechanism to sense the redox state of F420. The roles of the hydrogenases in
39 energy conservation during growth with each methanogenic pathway are discussed.

40

41 **IMPORTANCE**

42 Methanogenic archaea are key players in the global carbon cycle due to their
43 ability to facilitate the remineralization of organic substrates in many anaerobic
44 environments. The consequences of biological methanogenesis are far reaching,
45 with impacts on atmospheric methane and CO₂ concentrations, agriculture, energy
46 production, waste treatment and human health. The data presented here clarify the
47 *in vivo* function of hydrogenases during methanogenesis, which in turn deepens our
48 understanding of this unique form of metabolism. This knowledge is critical for a
49 variety of important issues ranging from atmospheric composition to human health.

50

51 **INTRODUCTION**

52 The ability to metabolize molecular hydrogen (H₂) is a key metabolic feature
53 in methanogenic Archaea (1). This trait is conferred by a class of enzymes known as
54 hydrogenases, which catalyze the reversible oxidation of H₂ coupled to various
55 electron donors/acceptors (2, 3). At least five distinct types of hydrogenases are
56 found in methanogenic archaea. These enzymes differ with respect to their redox
57 partners, their cellular localization, and whether their activity is linked to
58 production or consumption of membrane potential (4). Biochemical
59 characterization of these diverse hydrogenases led to proposed functions for each
60 enzyme class that differ substantially between methanogens with and without
61 cytochromes (5).

62 Methanogens without cytochromes produce at least four types of
63 hydrogenase; including (i) the electron-bifurcating Mvh hydrogenase, which couples
64 oxidation of hydrogen to reduction of ferredoxin and a mixed coenzyme M-
65 coenzyme B disulfide, (ii) the coenzyme F₄₂₀-dependent hydrogenase, (iii) the [Fe]
66 hydrogenase, which couples hydrogen oxidation to reduction of
67 methenyltetrahydromethanopterin, and (iv) the ferredoxin-dependent, energy-
68 converting hydrogenases (4). The first three are cytoplasmic enzymes, which supply
69 the electrons needed to reduce CO₂ to methane. The last is a membrane bound
70 multi-subunit complex that couples hydrogenase activity to the
71 production/consumption of the ion-motive force across the cell membrane (hence
72 the designation as “energy-converting”). In non-cytochrome-containing
73 methanogens, these energy-converting hydrogenases are believed to provide low-
74 potential electrons, in the form of reduced ferredoxin, needed for anaplerotic
75 reactions (6).

76 Methanogens with cytochromes, typified by *Methanosarcina barkeri*, encode
77 a different set of hydrogenases that includes one cytoplasmic and two membrane-
78 bound enzymes (Fig 1) (7). Like the non-cytochrome containing methanogens, *M.*
79 *barkeri* produces a cytoplasmic, three-subunit F₄₂₀-dependent hydrogenase known
80 as Frh (for F₄₂₀-reducing hydrogenase). Frh is encoded by the four-gene *frhADGB*
81 operon, which encodes the α , β and γ subunits (FrhA, FrhB and FrhG, respectively),
82 along with the maturation protease FrhD (8). A second locus, *freAEGB*, encodes
83 proteins that are 86-88% identical to FrhA, FrhB and FrhG, but lacks the gene for the
84 maturation protease FrhD, instead encoding a small protein of unknown function

85 (FrhE). It is not known whether the *fre* operon is capable of producing an active
86 hydrogenase (8-11). A membrane-bound hydrogenase linked to the quinone-like
87 electron carrier methanophenazine has, to date, been found only in *Methanosarcina*
88 species. This enzyme, known as Vht because it was initially identified as a viologen-
89 reducing hydrogenase, is encoded by the *vhtGACD* operon, which encodes the
90 biochemically characterized enzyme comprised of VhtA and VhtG, along with a
91 putative membrane-bound cytochrome, VhtC, that does not co-purify with the active
92 enzyme, and a maturation protease, VhtD (7). As with the F420-reducing
93 hydrogenase, a second locus that lacks the maturation protease is encoded in *M.*
94 *barkeri* strains. This operon (*vhxGAC*) encodes proteins that display *ca.* 50% amino
95 acid identity with those encoded by *vhtGACD*. Like *freAEGB*, it is not known whether
96 the *vhx* operon produces an active hydrogenase (7). Finally, *M. barkeri* encodes a
97 membrane-bound, ferredoxin-dependent energy-converting hydrogenase (Ech)
98 (12). This five-subunit enzyme complex is much simpler than, and only distantly
99 related to, the energy-converting hydrogenases of the non-cytochrome
100 methanogens, which typically contain more than a dozen subunits (3). Homologs of
101 the electron bifurcating- and methenyltetrahydromethanopterin-reducing
102 hydrogenases are not known to occur in cytochrome-containing methanogens.

103 A key difference between the cytochrome-containing and non-cytochrome-
104 containing methanogens is the ability of the former to use one-carbon (C-1)
105 compounds and acetic acid, in addition to H₂/CO₂, as growth substrates. Catabolism
106 of these chemically diverse substrates involves four distinct methanogenic
107 pathways: the CO₂ reduction pathway, the methyl reduction pathway, the

108 methylotrophic pathway and the aceticlastic pathway (13, 14). While several of
109 these pathways share common steps, they differ substantially with respect to
110 involvement of key enzymes and the direction of metabolic flux during methane
111 production (Fig 2). Surprisingly, it now appears that some *Methanosarcina* species
112 (e.g. *M. barkeri*) use hydrogenases in each of the four pathways, regardless of
113 whether external H₂ is provided as a growth substrate (15).

114 During the CO₂ reduction pathway, wherein CO₂ is reduced to CH₄ in a
115 stepwise manner, hydrogenases produce the electron-donating cofactors required
116 for four distinct reduction steps (Fig 2) (5). Initial reduction of CO₂ to formyl-
117 methanofuran requires reduced Fd (Fd_{red}), which is produced by Ech. This reaction
118 is dependent on ion-motive force because reduction of Fd by H₂ is endergonic under
119 physiological conditions (16). Subsequent reduction of methenyl-
120 tetrahydrosarcinapterin (H₄SPT) to methylene-H₄SPT, and of methylene-H₄SPT to
121 methyl-H₄SPT, requires reduced coenzyme F420 (F420_{red}), which is supplied by Frh.
122 Finally, reduction of a methyl group to methane using coenzyme B produces a
123 heterodisulfide of coenzyme M and coenzyme B (CoM-S-S-CoB), which must be
124 reduced to produce the free CoM and CoB needed for continued methanogenesis.
125 This reaction is catalyzed by a membrane bound heterodisulfide reductase (HdrED),
126 which uses the reduced form of a membrane-bound cofactor, methanophenazine, as
127 the source of electrons (17). H₂, in turn, serves as the reductant for generation of
128 reduced methanophenazine via membrane-bound Vht hydrogenase. Thus, all three
129 types of hydrogenase are predicted to be required for growth via CO₂ reduction, a

130 conclusion that has been validated by the phenotypic analysis of single mutants (11,
131 15, 16).

132 In contrast, methanogenesis via the methyl reduction pathway is expected to
133 require only Vht. In this pathway, methyl-CoM derived from C-1 compounds, such as
134 methanol or methylamines, is directly reduced to methane using CoB as the electron
135 donor. As with the CO₂ reduction pathway, this produces a CoM-S-S-CoB disulfide
136 that must be regenerated in a pathway requiring HdrDE and reduced
137 methanophenazine, which is presumably generated by Vht (Fig 2). This idea is
138 supported by the analysis of conditional *vht* mutants (15). Neither Frh nor Ech is
139 required for methanogenesis in this model, a finding that is consistent with
140 experimental data from Δfrh and Δech mutants (11, 16). Nevertheless, the *M. barkeri*
141 Δech strain cannot grow via the methyl reduction pathway unless the media are
142 supplemented with acetate and/or pyruvate. Thus, Ech plays an essential
143 biosynthetic role under these conditions, which is probably the H₂-dependent
144 synthesis of reduced ferredoxin needed for synthesis of acetyl-CoA and pyruvate
145 (16).

146 During acetoclastic methanogenesis, both the Ech and Vht hydrogenases play
147 a critical role in methanogenesis. In this pathway, acetyl-CoA is split into methyl-
148 H₄SPT and enzyme-bound [CO] by the acetyl-CoA decarbonylase/synthase (ACDS)
149 enzyme complex. CO is then further oxidized to CO₂ with concomitant reduction of
150 ferredoxin (12, 16). It is believed that the exergonic oxidation of ferredoxin by Ech
151 produces H₂ and contributes to the proton motive force by transferring protons
152 across the membrane. The proton motive force is further enhanced by a putative H₂

153 cycling mechanism, in which the H₂ produced by Ech diffuses across the membrane,
154 where it is oxidized by Vht to produce reduced methanophenazine. This unusual
155 electron transport chain is completed when the reduced methanophenazine
156 produced by Vht is used by HdrDE to regenerate free CoM and CoB from the CoM-S-
157 S-CoB heterodisulfide (Fig 2) (18). Participation of these hydrogenases in the
158 acetoclastic pathway is supported by mutagenic studies showing that *ech* and *vht*
159 mutants do not grow with acetate as the sole substrate, regardless of whether
160 biosynthetic precursors were supplied (15, 16).

161 Finally, all three types of hydrogenases are thought to be involved in
162 methylotrophic methanogenesis via a H₂ cycling mechanism similar to that
163 described for acetoclastic growth (15). In this pathway, F420_{red} and Fd_{red}, produced
164 by the stepwise oxidation of methyl groups to CO₂, are converted to molecular H₂ by
165 Frh and Ech, respectively (Fig 2). H₂ then diffuses to the outer surface of the cell
166 membrane where it is oxidized by Vht, releasing protons on the outside of the cell
167 and contributing to the generation of an ion-motive force (Fig 3) (15). Nevertheless,
168 *M. barkeri* Δ *frh* and Δ *ech* strains are capable of methylotrophic growth, indicating
169 the presence of alternative pathways for transfer of electrons from F420_{red} and Fd_{red}
170 to the electron transport chain (11, 16). The membrane-bound F420 dehydrogenase
171 complex (Fpo) has been identified as the alternate mechanism of electron transfer
172 from F420_{red} (11). This enzyme couples the exergonic reduction of
173 methanophenazine by F420_{red}, with the generation of proton motive force in a H₂
174 independent manner. However, the *M. barkeri* Δ *frh* strain exhibits slower growth
175 rates than wild type *M. barkeri*, showing that the H₂-independent electron transport

176 chain is less effective than electron transport via H₂ cycling. The observation that
177 $\Delta fpo/\Delta frh$ double mutants are incapable of methylotrophic growth shows that
178 additional electron transport routes are either not present, or not sufficient for
179 methylotrophic growth (11). Mutants lacking Vht are inviable under all growth
180 conditions, including methylotrophic growth, unless Frh is also removed. This
181 phenotype is probably due the inability to recapture H₂ produced in the cytoplasm,
182 which causes redox imbalance and cell lysis (15).

183 Although the three *M. barkeri* hydrogenases have been studied *in vitro* and in
184 certain mutants, a complete analysis of their role during growth on various
185 substrates has yet to be reported. In this study, all five hydrogenase operons were
186 systematically deleted in all viable combinations, and the physiological ramifications
187 of these mutations examined by measuring growth, methanogenesis and
188 hydrogenase activity on various growth substrates. We also performed global
189 transcriptional profiling to assess the possibility that alternate electron transport
190 chain components might be upregulated to compensate for the loss of specific
191 hydrogenases. The data suggest that hydrogenases are not required for
192 methylotrophic methanogenesis, but are essential for CO₂ reductive, methyl
193 reductive, and acetoclastic methanogenesis. Additionally, an inhibitory effect of H₂
194 on the methyl oxidative pathway appears to be mediated by all three hydrogenases.

195

196 **RESULTS**

197 **Construction of hydrogenase deletion mutants.** To assess the role of the *M.*
198 *barkeri* hydrogenases during growth on various substrates, we constructed mutants

199 lacking the *frhADGB*, *freAEGB*, *vhtGACD*, *vhxGAC* and *echABCDEF* operons,
200 individually and in all possible combinations (Fig S1). Because mutants lacking *vht*
201 are only viable in Δfrh mutants (15), we also created a series of conditional mutants
202 that have the *vht* promoter replaced by the synthetic P_{tet} promoter, which is
203 expressed in the presence of tetracycline and tightly repressed in its absence (19).
204 To simplify the isolation of strains lacking the adjacent *vht* and *vhx* loci, we
205 constructed a mutant allele (denoted $\Delta vht-vhx$) that deleted both operons along
206 with two intervening genes that encode a putative peptidoglycan binding protein
207 (Mbar_A1842) and an uncharacterized hypothetical protein (Mbar_A1843). The full
208 set of strains containing deletions for hydrogenase operons in all possible
209 combinations were successfully generated and verified by either Southern
210 hybridization or PCR (Figures S2-S5).

211 **Characterization of growth phenotypes in hydrogenase deletion**
212 **mutants.** The generation time, growth yield and duration of lag phase for each
213 mutant was determined by monitoring optical density during growth in a variety of
214 media, providing clues as to the function of each hydrogenase during utilization of
215 various carbon and energy sources (Table 1). With the exception of the Δfre and
216 Δvxh mutations, which had no discernable phenotypes alone or in combination with
217 other gene deletions, each of the mutations caused significant growth defects in one
218 or more media.

219 Strains containing the Δech mutation were unable to grow in either H_2/CO_2
220 or acetate media, regardless of whether the other hydrogenase genes were deleted.
221 However, with the exception of the $P_{tet}vht/\Delta ech$ mutant discussed below, these

222 mutants all grew on methanol medium, albeit with reduced growth rates. Consistent
223 with previous reports (16), the Δech single mutant was unable to grow on
224 unsupplemented methanol/H₂/CO₂ medium. Interestingly, the $\Delta ech/\Delta frh$ double
225 mutant regained the ability to grow in this medium, but with diminished rate and
226 yield and the longest lag phase observed in any of our experiments. These
227 phenotypes were substantially minimized in the $\Delta ech/\Delta frh/\Delta vht$ triple mutant,
228 suggesting that both Frh and Vht inhibit methanol oxidation, which is needed to
229 provide reducing equivalents for biosynthesis, when H₂ is present.

230 As previously reported, we were unable to obtain a mutant lacking only *vht*,
231 suggesting that loss of this locus is lethal in otherwise wild-type strains (15). This
232 conclusion was supported by the phenotype of the P_{tet}*vht* and P_{tet}*vht*/ Δech mutants,
233 which were incapable of growth on any medium when tetracycline is absent (*i.e.*
234 under repressing conditions). However, as previously noted, when cells were grown
235 on methanol it was possible to delete the *vht* operon if *frh* was deleted first. The
236 $\Delta frh/\Delta vht$ strains, including ones that also carried an *ech* deletion, had methanol
237 growth phenotypes similar to that of the wild type. Thus, hydrogenases are not
238 required for growth on methanol, although *vht*-deficient strains are inviable in the
239 presence of an active Frh hydrogenase. In contrast, strains lacking *vht* alone or in
240 combination with other mutations were unable to grow on either H₂/CO₂ or acetate
241 media. A more graded response was observed when various *vht* mutants were
242 grown on methanol/H₂/CO₂. Accordingly, on this substrate combination, the *vht*
243 single mutant was inviable, while the $\Delta frh/\Delta vht$ double mutant grew very poorly
244 and the $\Delta ech/\Delta frh/\Delta vht$ strain had phenotypes that were nearly wild-type. Again,

245 these data are consistent with the idea that with certain mutant backgrounds Frh,
246 Vht and Ech inhibit methanol oxidation in the presence of H₂.

247 Finally, mutants lacking only the *frh* operon grew on three out of four
248 substrates tested, failing to grow only on H₂/CO₂ medium. When methanol was the
249 sole substrate, the Δfrh mutant had an extended lag phase and a generation time
250 approximately double that of the parental strain. However, during growth on either
251 acetate or methanol/H₂/CO₂ the growth phenotypes of this strain were equivalent
252 to the parental strain, suggesting Frh enhances growth on methanol, but is not
253 required for growth on the two latter substrate combinations.

254 **Methane and CO₂ production by hydrogenase deletion mutants.** To
255 probe the underlying mechanisms behind the growth phenotypes, we also examined
256 production of methane and CO₂ by resting cell suspensions incubated with various
257 substrates (Tables 2 & 3). The P_{tet}*vht* and P_{tet}*vht*/ Δech mutants were not examined
258 because they do not grow in any medium under non-inducing conditions. Similarly,
259 we did not assay production of methane from acetate, because prior growth on
260 acetate is required to induce the enzymes needed for this activity and most of the
261 hydrogenase mutants are unable to grow under these conditions (20, 21).

262 Consistent with their lack of growth phenotypes, the Δfre and Δvhx single
263 mutations did not affect the levels of methane produced from any substrate tested.
264 Neither did these mutations affect the ratio of methane/CO₂ produced from
265 methanol or from methanol/H₂. However, the Δvhx mutation slowed the rate of
266 methane production. The Δfre mutation also slowed the rate of methane production,
267 but only when combined with the Δfrh mutation.

268 As seen in previous studies, Δech mutants produced only minor amounts of
269 methane from H_2/CO_2 (<2% relative to the parental strain), but produced wild-type
270 levels from both methanol and methanol/ H_2 . During incubations with methanol,
271 methane and CO_2 were produced in a 3:1 ratio, consistent with disproportionation
272 of the substrate via the methylotrophic pathway (Fig 2). Cell suspensions incubated
273 with methanol and H_2 produced only methane, showing that addition of hydrogen
274 inhibits methanol oxidation. The rate of methane production by the Δech mutant
275 was somewhat slower than wild-type using both methanol and methanol/ H_2 . This
276 rate was further reduced when the *ech* deletion was combined with mutations
277 removing the *frh* or *vht* operons. Accordingly, the $\Delta ech/\Delta frh$ double mutant
278 produced methane nearly 5 times slower than the wild-type strain. Interestingly,
279 this mutant produced a small amount of CO_2 in addition to the wild-type level of
280 methane, indicating a small amount of methanol was oxidized. When the *ech*, *frh*,
281 and *vht* hydrogenases were deleted together, the quantity and stoichiometry of
282 methane and CO_2 production was identical to that observed on methanol alone.

283 The Δfrh single mutant produced similar levels and ratios of methane and
284 CO_2 relative to the parental strain with methanol or methanol/ H_2 . When H_2/CO_2 was
285 the substrate, methane production was reduced *ca.* 10-fold, but, significantly, not
286 abolished. Combining the Δfrh mutation with deletions of *vht* and *ech* reduced
287 methane production from H_2/CO_2 to negligible levels. In contrast, minimal affects on
288 methane and CO_2 production or stoichiometry were observed when methanol was
289 the sole substrate. However, when combined with deletions of *vht* or *ech*, the Δfrh
290 mutants produced significant levels of CO_2 when incubated with methanol/ H_2 , and

291 the triple $\Delta ech/\Delta frh/\Delta vht$ mutant produced similar levels to that seen in assays
292 incubated with methanol alone. Rates of methane production were substantially
293 slower than wild-type for all Δfrh mutants.

294 **Enzyme activity in hydrogenase mutants.** The hydrogenase activity for
295 selected deletion mutants was measured in the forward direction (H_2 oxidation) to
296 allow estimation of the contributions of each enzyme to overall activity (Table 4).

297 The hydrogenase activity of mutants lacking Fre or Vhx was not statistically
298 different from the parental strain. Moreover, hydrogenase activity of the
299 $\Delta ech/\Delta frh/\Delta vht$ mutant, which still encodes Fre and Vhx, was not statistically
300 different than the $\Delta ech/\Delta frh/\Delta fre/\Delta vht-vhx$ mutant that lacks all five hydrogenase
301 operons. Thus, the *freAEGB* and *vhxGAC* operons do not, by themselves, produce
302 detectable levels of hydrogenase. Because Fre and Vhx are essentially inactive, the
303 hydrogenase levels in the $\Delta frh/\Delta vht$ and $\Delta ech/\Delta frh$ strains can be attributed solely
304 to Ech and Vht, respectively. Accordingly, Ech has the lowest activity of the three
305 hydrogenases, accounting for *ca.* 4% of total activity, and with Vht activity being *ca.*
306 6-fold higher. Consistent with this conclusion, deletion of *ech* did not significantly
307 affect hydrogenase activity, whereas the Δfrh strain had drastically diminished
308 activity as compared to the parental strain. Additionally, activity from the Δfrh
309 strain, which encodes both Vht and Ech, is roughly equivalent to the combined
310 activities of strains encoding only Vht or only Ech. Because strains expressing only
311 Frh hydrogenase are inviable, the activity of this hydrogenase cannot be directly
312 determined from a mutant strain. However, the relative contribution of Frh can be
313 estimated from the hydrogenase activities of other mutants. Thus, by subtracting

314 the activities of Vht and Ech from that of the parental strain, we estimate that
315 roughly 75% of hydrogenase activity can be attributed to Frh.

316 **Effect of hydrogenase deletions on mRNA abundance.** Our estimate of the
317 relative activities of the individual hydrogenases assumes that the expression levels
318 for each hydrogenase are unaffected by deletion of the others. To explicitly examine
319 this possibility, we determined the global mRNA abundance profiles for each mutant
320 using RNA seq (Table S4 and Dataset S1). Importantly, the RNA used in this analysis
321 was isolated from the same cultures that were assayed for hydrogenase activity.

322 As expected, the mRNA levels for the deleted genes in each mutant were
323 significantly and substantially lower than the parental strain, providing an
324 important validation that the correct strains were used in these assays. Moreover,
325 no significant differences in mRNA abundance from the parent were observed for
326 the remaining hydrogenases in any strain, showing that the expression of individual
327 hydrogenase operons is not regulated by the presence/absence of other
328 hydrogenase genes. Thus, the hydrogenase activities found in the various mutants
329 accurately reflect the combined activities of each enzyme in all strains.

330 Large numbers of *M. barkeri* genes showed significant changes in mRNA
331 abundance in the hydrogenase mutants, relative to the parental strain. Accordingly,
332 2.7% of all genes were differently regulated in strains with one or two deleted
333 hydrogenases, whereas the $\Delta ech/\Delta frh/\Delta vht$ and $\Delta ech/\Delta frh/\Delta fre/\Delta vht-vhx$ strains
334 showed in 17.4% and 22.5% differently regulated genes, respectively (Dataset S1).
335 Of these, most encode proteins with unknown functions or with annotated functions
336 that do not appear to be related to energy conservation. One exception was the F420

337 dehydrogenase (*fpo*), whose mRNA abundance increased significantly in all strains
338 lacking *frh* (Table S4). This result suggests that the cell has a mechanism to sense
339 the redox state of F420, which is altered upon deletion of *frh*.

340

341 **DISCUSSION**

342 While fully consistent with the proposed functions of the *M. barkeri*
343 hydrogenases, our phenotypic characterization of mutants lends new insight into
344 the flexibility and interconnected nature of methanogenic metabolism. For example,
345 reduction of CO₂ to CH₄ is expected to require three kinds of electron donors: Fd_{red},
346 F420_{red}, and reduced methanophenazine (1). Consistent with this idea, mutants
347 lacking hydrogenases that reduce Fd (Ech), F420 (Frh) or methanophenazine (Vht)
348 are unable to grow on H₂/CO₂. Thus, we were surprised to observe production of
349 methane from H₂/CO₂ in cell suspensions of Δ *frh* mutants. Assuming this process
350 involves the standard CO₂ reduction pathway, this would require an alternative
351 source of F420_{red} for reduction of methenyl- and methylene-tetrahydrosarcinapterin
352 (Fig 2). Two alternative sources can be envisioned: first, Fpo could produce F420_{red}
353 using reduced methanophenazine as the electron donor via reverse electron
354 transport driven by proton motive force; second, a soluble heterodisulfide reductase
355 could produce F420_{red} via electron bifurcation using CoM-S-S-CoB and Fd_{red} as
356 substrates (as suggested in (22, 23)). In the former mechanism, reduced
357 methanophenazine would be derived from H₂ using Vht; in the latter, Fd_{red} would be
358 derived from H₂ via Ech. Interestingly, double mutants lacking Frh and either Ech or
359 Vht produce much less methane than the Δ *frh* single mutant, thus both alternate

360 pathways may contribute to this phenotype. The inability of the Δfrh mutant to grow
361 on H_2/CO_2 suggests that this alternate methane-producing pathway does not
362 provide sufficient energy for growth, or that it fails to provide an essential
363 biosynthetic precursor.

364 Similar metabolic flexibility is seen during methylotrophic methanogenesis,
365 which can occur via H_2 -dependent or -independent mechanisms (Figures 2, 3) (11,
366 12, 15, 16). We previously showed that a hydrogen cycling mechanism involving Frh
367 and Vht is the preferred mode of electron transport in *M. barkeri*. Nevertheless, *M.*
368 *barkeri* is also capable of methylotrophic growth in the absence of Frh and Vht (11,
369 15). Data reported here reveal that methylotrophic growth in *M. barkeri* is possible
370 when all three hydrogenases are deleted. Thus, we have created an *M. barkeri* strain
371 similar to *Methanosarcina acetivorans*, which has no detectable hydrogenase activity,
372 but which grows well on methylotrophic substrates (7, 14). During methylotrophic
373 growth in *M. acetivorans*, an electron transport chain comprised of Fpo and HdrDE is
374 used to capture energy from $F420_{red}$ produced by the oxidative branch of the
375 methanogenic pathway (Figures 2, 3). Our genetic analyses suggest that Fpo is also
376 used to metabolize $F420_{red}$ in *M. barkeri* $\Delta frh/\Delta vht$ mutants (11, 15). The oxidative
377 branch of the methylotrophic pathway also produces Fd_{red} , which in *M. acetivorans*
378 is oxidized by membrane-bound, ion-pumping Fd_{red} :methanophenazine
379 oxidoreductase known as Rnf (24). However, because *M. barkeri* does not encode
380 Rnf, this energy-conserving electron transport pathway is not available to the Ech
381 mutants characterized here. Thus, an alternative Fd_{red} :heterodisulfide
382 oxidoreductase system must exist to allow growth of these mutants on methanol. It

383 has been suggested that this alternate Fd_{red} :heterodisulfide oxidoreductase activity
384 is catalyzed by a cytoplasmic, electron-bifurcating heterodisulfide reductase
385 (HdrABC), similar to the electron-bifurcating heterodisulfide reductase of non-
386 cytochrome containing methanogens (Fig 3) (22). Biochemical data from a
387 homologous *M. acetivorans* enzyme supports this possibility (23).

388 Interestingly, the stoichiometry of methane and CO_2 produced from
389 methanol/ H_2 in $\Delta frh/\Delta vht$ and $\Delta frh/\Delta fre/\Delta vht-vhx$ mutants lends additional support
390 for an alternate Fd_{red} :heterodisulfide oxidoreductase. These strains, which encode
391 only Ech, might be expected to disproportionate methanol to CH_4 and CO_2 in a 3:1
392 ratio, as was seen in the strains lacking all three active hydrogenases. Instead, they
393 produced CH_4 and CO_2 at an approximate ratio of 10:1, suggesting that a substantial
394 portion of methanol was reduced directly to CH_4 using electrons obtained by H_2
395 oxidation. Because Ech is the sole remaining hydrogenase in these strains, electrons
396 from Fd_{red} must be involved in this process.

397 H_2 also inhibits oxidation of methanol when both substrates are present, via
398 a mechanism that is clearly mediated by hydrogenase activity. Accordingly, in the
399 presence of H_2 , methanol is solely reduced to methane by cell suspensions of strains
400 that contain all three hydrogenases, while it is disproportionated to methane and
401 CO_2 in a 3:1 ratio when all three are absent. The hydrogenase-mediated inhibition of
402 methanol oxidation is graded, with Vht having the largest effect and Ech the least.
403 Similarly, Ech mutants are only able to grow on methanol/ H_2 when supplemented
404 with acetate and pyruvate, which has been interpreted to mean they cannot produce
405 the reducing equivalents needed for biosynthesis by oxidizing methanol to CO_2 (16).

406 We showed here that this effect is alleviated by deletion of genes encoding Frh and
407 Vht, with the Δvht mutation having a much larger effect. Because protein synthesis
408 was blocked by addition of puromycin in the cell suspension experiments, these
409 effects cannot have been mediated by changes in the concentration of enzymes in
410 the methanogenic pathways. Moreover, because inhibition requires the
411 hydrogenase enzymes to be present, it is likely that a product of the enzymatic
412 reaction mediates inhibition: namely the reduced enzyme cofactors. Thus, in the
413 presence of high H_2 partial pressures and the appropriate hydrogenase, we would
414 expect the levels of oxidized methanophenazine, $F420_{ox}$ and Fd_{ox} to be kept at very
415 low levels. Interestingly, the graded inhibition in response to loss of Vht, Frh and
416 Ech mimics the thermodynamics of the hydrogenase reactions, with
417 methanophenazine being the most energetically favorable electron acceptor and Fd
418 being the least. This suggests at least two possible mechanisms that might account
419 for the inhibition: *i*) allosteric inhibition or covalent inactivation of a key enzymatic
420 step in the oxidative branch of the pathway could be triggered by one or more
421 reduced cofactors, or *ii*) simple changes in the availability of $F420_{ox}$ and Fd_{ox} , which
422 are needed for three discrete steps in the oxidative branch of the methyloptrophic
423 pathway (Fig 2). Note that in the second mechanism, the major inhibitory effect of
424 Vht on methyl oxidation can only be explained if high levels of reduced
425 methanophenazine influence the levels of $F420_{ox}$, which could occur by changing the
426 equilibrium of the Fpo reaction (Fig 2, 3).

427 In addition to affecting flux through methanogenic pathways, the levels of
428 reduced or oxidized cofactors may be used as a sensory input to modulate gene

429 regulation. Transcriptional profiling of hydrogenase mutants showed that in all
430 strains lacking *frh*, the *fpo* operon was significantly up-regulated. Without Frh, Fpo
431 is solely responsible for the F420_{red}:methanophenazine oxidoreductase activity
432 required to transfer electrons from the oxidative to reductive portions of the
433 methylotrophic electron transport pathway. Elevated abundance of *fpo* mRNA in
434 Δfrh strains indicates that the cell has a mechanism to sense and respond to F420
435 redox imbalance. A previous study identified MreA as a global regulator in
436 *Methanosarcina* with the ability to bind and repress the *fpo* promoter region during
437 acetoclastic growth (25). This regulator was shown to affect gene expression based
438 on growth substrate, however the mechanism and sensory input are unknown.
439 Systems for gene regulation based on detected redox imbalance of F420 and other
440 electron carriers are a potential source for future studies.

441 The levels of hydrogenase activity for the three enzyme types have
442 significant ramifications for the hydrogen cycling model on energy conservation
443 (15). We have shown that Δvht mutations are lethal when Frh is present, but not
444 when it is absent. Moreover, when *vht* expression is turned off using a regulated
445 promoter, cell lysis is concomitant with H₂ accumulation, implying that the inability
446 to recapture H₂ produced in the cytoplasm is responsible for the lethal phenotype.
447 With this in mind, it seems clear that the cytoplasmic activities of Frh must be
448 carefully balanced against the periplasmic activity of Vht. Interestingly, our data
449 show that Frh activity is ca. 3-fold higher than that of Vht. Thus, it appears that
450 ability of Frh to produce H₂ is much higher than the ability of Vht to take it up. We
451 recognize that our assays were not conducted with the native substrates (which are

452 not commercially available), therefore we approximated the *in vivo* activity of each
453 enzyme based on available literature values in which a variety of natural and
454 artificial cofactors were used (Table S5). These data suggest that the relative
455 activities of Frh and Vht are more similar than our assay data suggest, with Frh
456 activity ca. 1.5-fold higher than Vht. While this extrapolation must be interpreted
457 with caution, it still suggests that Frh capacity is higher than that of Vht. In this
458 regard, both Vht and Ech are coupled to ion-motive force; thus, activity in whole,
459 metabolically active cells could be substantially different.

460 Finally, unlike Frh and Vht, Fre and Vhx are not able to provide sufficient
461 levels of F420_{red} and reduced methanophenazine, respectively, for growth via CO₂
462 reduction. Additionally, the $\Delta ech/\Delta frh/\Delta vht$ strain that only encoded for the Fre and
463 Vhx hydrogenases had no detectable hydrogenase activity. This could be due to low
464 expression of *fre* and *vhx* operons, absence of post-translational processing,
465 mutations in structural or catalytic residues or some combination of these (7).
466 Analysis of RNA sequencing data from wild type *M. barkeri* grown
467 methylo-trophically indicated the abundance mRNA for *fre* approximately 50-lower
468 than *frh* (Dataset S1), similar to the relative abundance observed by Vaupel and
469 Thauer (8). Additionally, the abundance of *vhx* transcripts was more than 200-fold
470 lower than those of *vht*. We note that our enzymatic assays would have easily
471 detected hydrogenase activity at levels 200-fold lower than we observed for the
472 strains encoding only *vht*. Thus, poor gene expression cannot explain the lack of
473 activity in strains expressing only Fre or Vhx. Hydrogenases require several
474 maturation steps to become active enzymes, including processing by the maturation

475 proteases encoded by the *frhD* and *vhtD* genes. Thus, it remains possible that Fre
476 and Vhx could encode active enzymes if FrhD and VhtD are *trans*-acting maturation
477 proteases. Given that the mutants characterized here removed the entire *frh* and *vht*
478 operons, our data do not address this possibility.

479

480 **MATERIALS AND METHODS**

481 **Media and growth conditions**

482 *Methanosarcina* strains were grown as single cells (26) at 37 °C in high salt
483 (HS) broth medium (27) or on agar-solidified medium as described (28). Growth
484 substrates provided were methanol (125 mM in broth medium and 50 mM in agar-
485 solidified medium) or sodium acetate (120 mM) under a headspace of N₂:CO₂ (80:20
486 v/v) at 50 kPa over ambient pressure, H₂:CO₂ (80:20 v/v) at 300 kPa over ambient
487 pressure, or a combination of methanol plus hydrogen. Cultures were supplemented
488 as indicated with 0.1% yeast extract (YE), 0.1% casamino acids (CAA), 10 mM
489 sodium acetate, 10 mM pyruvate or 100 mM pyruvate. Puromycin (CalBioChem, San
490 Diego, CA) was added at 2 mg ml⁻¹ for selection of the puromycin transacetylase
491 (*pac*) gene (29). 8-Aza-2,6-diaminopurine (8-ADP) (Sigma, St Louis, MO) was added
492 at 20 mg ml⁻¹ for selection against the presence of *hpt* (29). Tetracycline (Tc) was
493 added at 100 mg ml⁻¹ to induce the tetracycline-regulated *PmcrB(tetO1)* promoter
494 (19). Standard conditions were used for growth of *Escherichia coli* strains (30)
495 DH5α/*λ-pir* (31) and DH10B (Stratagene, La Jolla, CA), which were used as hosts for
496 plasmid constructions.

497 **DNA methods and plasmid constructions**

498 Standard methods were used for plasmid DNA isolation and manipulation in
499 *E. coli* (32). Liposome mediated transformation was used for *Methanosarcina* as
500 described (33). Genomic DNA isolation and DNA hybridization were as described
501 (27, 28, 34). DNA sequences were determined from double-stranded templates by
502 the W.M. Keck Center for comparative and functional genomics, University of Illinois.
503 Plasmid constructions are described in Tables S1 and S2.

504 **Strain construction in *M. barkeri***

505 The construction and genotype of all *Methanosarcina* strains is presented in
506 Table S3. Hydrogenase encoding genes were deleted sequentially in a specific order
507 (Figure S1) because certain hydrogenase deletion mutants are only viable when
508 other hydrogenase genes are deleted first (15). To simplify isolation of strains that
509 lack hydrogenase operons *vhxGAC* and *vhtGACD*, the genes between the two operons
510 (*Mbar_A1842* and *Mbar_A1843*) were also deleted (Figure 1). All mutants were
511 confirmed by either PCR or DNA hybridization (Figures S2-S5).

512 **Determination of growth characteristics**

513 For growth rate determinations, cultures were grown on methanol or
514 methanol plus H₂/CO₂ (Δ *frh* and Δ *frh*/ Δ *fre*) to mid-log phase (optical density at 600
515 nm [OD₆₀₀] *ca.* 0.5). Approximately 3% inoculum of the culture (or 10%, in case of
516 acetate) was then transferred to fresh medium in at least four replicates and
517 incubated at 37 °C. Growth was quantified by measuring OD₆₀₀. With the exception
518 of samples grown on acetate, all OD₆₀₀ were measured with a Spectronic 20
519 spectrophotometer (Thermo Fisher Scientific, Waltham, MA); those grown on
520 acetate were measured with a Hewlett Packard 8453 spectrophotometer (Agilent,

521 Santa Clara, CA). Note that an OD of 1.0 on the Hewlett Packard 8453 is equivalent to
522 an OD of ~0.2 on the Spectronic 20. Generation times were calculated during
523 exponential growth phase and lag phase was defined as the time required to reach
524 half-maximal OD₆₀₀.

525 **Cell suspension experiments**

526 Cells grown on methanol or methanol plus H₂/CO₂ (Δfrh and $\Delta frh/\Delta fre$) were
527 collected in late exponential phase (OD₆₀₀ = 0.6-0.7) by centrifugation at 5,000 x g
528 for 15 minutes at 4 °C. The cells were washed once with anaerobic HS PIPES buffer
529 (50 mM PIPES at pH 6.8, 400 mM NaCl, 13 mM KCl, 54 mM MgCl₂, 2 mM CaCl₂, 2.8
530 mM cysteine, 0.4 mM Na₂S) and resuspended in the same buffer to a final
531 concentration of 10⁹ cells/ml. Cells were counted visually using the Petroff-Hausser
532 counting chamber (Hausser Scientific, PA). All assay mixtures contained 2 ml of the
533 suspension and were conducted under strictly anaerobic conditions in 25 ml Balch
534 tubes sealed with butyl rubber stoppers using 250 mM methanol as the
535 methanogenic substrate under a headspace of N₂, H₂, or H₂/CO₂ (80/20%) at 250
536 kPa over the ambient pressure, as indicated. Puromycin (20 µg/ml) was added to
537 prevent protein synthesis. Cells were held on ice until initiation of assay by transfer
538 to 37 °C. For rate determination, gas phase samples were withdrawn at various time
539 points and assayed for CH₄ by gas chromatography at 225 °C in a Hewlett Packard
540 gas chromatograph (5890 Series II) equipped with a flame ionization detector. The
541 column used was stainless steel filled with 80/120 Carbopack™ B/3% SP™-1500
542 (Supelco, Bellefonte, PA) with helium as the carrier gas. For total CH₄ and CO₂
543 production, assays were incubated at 37 °C for 36 hours prior to withdrawal of gas

544 phase samples for analysis by GC at 225 °C in a Hewlett Packard gas chromatograph
545 (5890 Series II) equipped with a thermal conductivity detector. A stainless steel
546 60/80 Carboxen-1000 column (Supelco, Bellefonte, PA) with helium as the carrier
547 gas was used. Total cell protein was determined using the Bradford method (35)
548 after 1 ml of the cells was lysed by resuspension in ddH₂O with 1 mg/ml RNase and
549 DNase.

550 **Hydrogenase assays**

551 Strains were grown at 37 °C in HS medium supplemented with 125 mM
552 methanol and cells were harvested from 10 ml mid-exponential phase culture at
553 1228 x *g* for 15 min in an IEC MediSpin (Needham Heights, MA) benchtop centrifuge.
554 Preparation of cell extract was performed in an anaerobic chamber under an
555 atmosphere of H₂/N₂ (4/96%). Cells were washed once in 10 ml HS-MOPS [2 mM
556 dithiothreitol (DTT), 400 mM NaCl, 13 mM KCl, 54 mM MgCl₂, 2 mM CaCl₂, 50 mM
557 MOPS, pH 7.0] and lysed in 1 ml lysis buffer (2 mM DTT, 0.5% *n*-dodecyl β-D-
558 maltoside, *ca.* 50 Kunitz units bovine pancreas deoxyribonuclease I, 50 mM MOPS,
559 pH 7.0) on ice for 30 min. Enzyme-containing supernatant was separated from cell
560 debris by centrifugation at 13600 x *g* for 2.5 min (Fisher Scientific Micro Centrifuge
561 Model 235C, Waltham, MA). Protein concentration was measured via the Bradford
562 method (35).

563 Assays were performed anaerobically in 1.7 ml quartz cuvettes sealed with
564 rubber stoppers. A total reaction volume of 1 ml was used, and included cell extract
565 mixed with 50 mM MOPS buffer (pH 7.0) containing 2 mM DTT and 2 mM benzyl
566 viologen (BV). The cuvette headspace was pressurized to 30 kPa with 100% H₂ after

567 being flushed for 2 min. Cuvettes with reaction mixture were pre-warmed to 30 °C
568 before the reaction was initiated by the addition of BV. Hydrogenase activity was
569 determined by quantifying the change in absorbance of BV at 578 nm (extinction
570 coefficient, 8.65 cm⁻¹ mM⁻¹) with a Cary 50 UV-Vis Spectrophotometer (Agilent,
571 Santa Clara, CA). One unit (U) of hydrogenase activity was defined as the oxidation
572 of 1 μmol H₂ per minute, based on the fact that 2 μmol BV are reduced for each H₂
573 oxidized. A minimum of three independent measurements from biological replicates
574 was performed for each strain.

575 **RNA sequencing**

576 Immediately prior to cell harvest for hydrogenase assays, 2.5 ml of the same
577 culture was harvested for total RNA isolation. An equal volume of TRIzol reagent
578 (Ambion, Carlsbad, CA) was added to the culture to lyse cells and samples were
579 incubated at room temperature for 5 min. RNA was then isolated with a Direct-zol
580 RNA MiniPrep kit from Zymo Research (Irvine, CA) according to the manufacturer's
581 directions. RNA samples were stored at -80 °C.

582 To increase coverage of mRNA during sequencing, rRNA was removed from
583 samples via subtractive hybridization. The method of Stewart et al. (36) was utilized
584 with the following modifications. Templates for 16S and 23S rRNA probes were
585 generated by PCR from strain WWM85 with primers 16SFor, T716SRev, 23SFor, and
586 T723SRev. *In vitro* transcription with the MEGAscript High Yield Transcription kit
587 (Ambion) was used for the production of biotinylated antisense rRNA probes from
588 400 ng of the purified PCR products in separate reactions. After removal of template
589 with DNaseI, probes were purified with the Zymo Research RNA Clean &

590 Concentrator kit. Hybridization reactions (30 μ l) for each sample contained the
591 following: 20% formamide, 1X SSC buffer, 20 U SUPERase inhibitor, 2 μ g total RNA,
592 4 μ g 16S probe, and 4 μ g 23S probe. Reactions were denatured at 70 $^{\circ}$ C for 10 min,
593 ramped down to 25 $^{\circ}$ C (-0.1 $^{\circ}$ C sec⁻¹), and incubated at room temperature for 10 min.
594 rRNA hybridized to biotinylated probe was removed via streptavidin-coated
595 magnetic beads (New England Biolabs, Ipswich, MA). Beads (500 μ l per sample)
596 were washed twice with 500 μ l 1X SSC buffer prior to the addition of hybridized
597 RNA sample diluted to 250 μ l in 1X SSC buffer with 20% formamide. Samples were
598 incubated for 1 hour at room temperature with gentle shaking before separation of
599 beads on a magnetic rack. The supernatant was removed, beads were washed with
600 250 μ l 1X SSC, and supernatant and wash were pooled and cleaned with the Zymo
601 Research RNA Clean & Concentrator kit.

602 Preparation and sequencing of RNAseq libraries was performed at the Roy J.
603 Carver Biotechnology Center at the University of Illinois at Urbana-Champaign.
604 Libraries were made with the TruSeq Stranded mRNA Sample Prep kit, sequenced
605 with a HiSeq 2000 using the TruSeq SBS v3 kit, and processed with Casava 1.8.2, all
606 per the manufacturer's directions (Illumina, San Diego, CA). All sequencing data was
607 further processed and analyzed as previously described (37) with CLC Genomics
608 Workbench 7 (Qiagen). Within this program, the Empirical analysis of Differential
609 Gene Expression (EDGE) tool was used for statistical analysis (38). Differently
610 regulated genes were considered significant when up- or down-regulated at least 3-
611 fold with a p-value \leq 0.05. Three biological replicates were sequenced and analyzed

612 for each strain. Raw and processed data have been deposited in the Gene Expression
613 Omnibus (GEO) under the accession number GSE98441.

614

615 **ACKNOWLEDGEMENTS**

616 The authors acknowledge the Division of Chemical Sciences, Geosciences, and
617 Biosciences, Office of Basic Energy Sciences of the U.S. Department of Energy
618 through Grant DE-FG02-02ER15296 for funding of this work.

619 **REFERENCES**

- 620 1. Thauer RK, Hedderich R, Fischer R. 1993. Reactions and Enzymes Involved in
621 Methanogenesis from CO₂ and H₂, p 209-252. *In* Ferry JG (ed),
622 Methanogenesis: Ecology, Physiology, Biochemistry & Genetics. Chapman &
623 Hall, New York, NY.
- 624 2. Vignais PM, Billoud B, Meyer J. 2001. Classification and phylogeny of
625 hydrogenases. *FEMS Microbiol Rev* 25:455-501.
- 626 3. Peters JW, Schut GJ, Boyd ES, Mulder DW, Shepard EM, Broderick JB, King PW,
627 Adams MWW. 2015. [FeFe]- and [NiFe]-hydrogenase diversity, mechanism,
628 and maturation. *Biochim Biophys Acta* 1853:1350-1369.
- 629 4. Thauer RK, Kaster A-K, Goenrich M, Schick M, Hiromoto T, Shima S. 2010.
630 Hydrogenases from methanogenic archaea, nickel, a novel cofactor, and H₂
631 storage. *Annu Rev Biochem* 79:507-536.
- 632 5. Thauer RK, Kaster A-K, Seedorf H, Buckel W, Hedderich R. 2008.
633 Methanogenic archaea: ecologically relevant differences in energy
634 conservation. *Nat Rev Microbiol* 6:579-591.
- 635 6. Lie TJ, Costa KC, Lupa B, Korpole S, Whitman WB, Leigh JA. 2012. Essential
636 anaplerotic role for the energy-converting hydrogenase Eha in
637 hydrogenotrophic methanogenesis. *Proc Natl Acad Sci U S A* 109:15473-
638 15478.
- 639 7. Guss AM, Kulkarni G, Metcalf WW. 2009. Differences in hydrogenase gene
640 expression between *Methanosarcina acetivorans* and *Methanosarcina barkeri*.
641 *J Bacteriol* 191:2826-2833.

- 642 8. Vaupel M, Thauer RK. 1998. Two F₄₂₀-reducing hydrogenases in
643 *Methanosarcina barkeri*. Arch Microbiol 169:201-205.
- 644 9. Fiebig K, Friedrich B. 1989. Purification of the F₄₂₀-reducing hydrogenase
645 from *Methanosarcina barkeri* (strain Fusaro). Eur J Biochem 184:79-88.
- 646 10. Michel R, Massanz C, Kostka S, Richter M, Fiebig K. 1995. Biochemical
647 characterization of the 8-hydroxy-5-deazaflavin-reactive hydrogenase from
648 *Methanosarcina barkeri* Fusaro. Eur J Biochem 233:727-735.
- 649 11. Kulkarni G, Kridelbaugh DM, Guss AM, Metcalf WW. 2009. Hydrogen is a
650 preferred intermediate in the energy-conserving electron transport chain of
651 *Methanosarcina barkeri*. Proc Natl Acad Sci U S A 106:15915-15920.
- 652 12. Meuer J, Bartoschek S, Koch J, Kunkel A, Hedderich R. 1999. Purification and
653 catalytic properties of Ech hydrogenase from *Methanosarcina barkeri*. Eur J
654 Biochem 265:325-335.
- 655 13. Liu Y, Whitman WB. 2008. Metabolic, Phylogenetic, and Ecological Diversity
656 of the Methanogenic Archaea. Ann N Y Acad Sci 1125:171-189.
- 657 14. Guss AM, Mukhopadhyay B, Zhang JK, Metcalf WW. 2005. Genetic analysis of
658 *mch* mutants in two *Methanosarcina* species demonstrates multiple roles for
659 the methanopterin-dependent C-1 oxidation/reduction pathway and
660 differences in H₂ metabolism between closely related species. Mol Microbiol
661 55:1671-1680.
- 662 15. Kulkarni G, Mand TD, Metcalf WW. 2018. Energy conservation via hydrogen
663 cycling in the methanogenic archaeon *Methanosarcina barkeri*. bioRxiv
664 <https://doi.org/>.

- 665 16. Meuer J, Kuettner HC, Zhang JK, Hedderich R, Metcalf WW. 2002. Genetic
666 analysis of the archaeon *Methanosarcina barkeri* Fusaro reveals a central role
667 for Ech hydrogenase and ferredoxin in methanogenesis and carbon fixation.
668 Proc Natl Acad Sci U S A 99:5632-5637.
- 669 17. Deppenmeier U. 2004. The membrane-bound electron transport system of
670 *Methanosarcina* species. J Bioenerg Biomembr 36:55-64.
- 671 18. Welte C, Deppenmeier U. 2014. Bioenergetics and anaerobic respiratory
672 chains of acetoclastic methanogens. Biochim Biophys Acta 1837:1130-1147.
- 673 19. Guss AM, Rother M, Zhang JK, Kulkarni G, Metcalf WW. 2008. New methods
674 for tightly regulated gene expression and highly efficient chromosomal
675 integration of cloned genes for *Methanosarcina* species. Archaea 2:193-203.
- 676 20. Krzycki JA, Wolkin RH, Zeikus JG. 1982. Comparison of unitrophic and
677 mixotrophic substrate metabolism by acetate-adapted strain of
678 *Methanosarcina barkeri*. J Bacteriol 149:247-254.
- 679 21. Jablonski PE, DiMarco AA, Bobik TA, Cabell MC, Ferry JG. 1990. Protein
680 content and enzyme activities in methanol- and acetate-grown
681 *Methanosarcina thermophila*. J Bacteriol 172:1271-1275.
- 682 22. Buan NR, Metcalf WW. 2010. Methanogenesis by *Methanosarcina acetivorans*
683 involves two structurally and functionally distinct classes of heterodisulfide
684 reductase. Mol Microbiol 75:843-853.
- 685 23. Yan Z, Wang M, Ferry JG. 2017. A Ferredoxin- and F₄₂₀H₂-Dependent,
686 Electron-Bifurcating, Heterodisulfide Reductase with Homologs in the
687 Domains Bacteria and Archaea. mBio 8: e02285-16.

- 688 24. Li Q, Li L, Rejtar T, Lessner DJ, Karger BL, Ferry JG. 2006. Electron transport
689 in the pathway of acetate conversion to methane in the marine archaeon
690 *Methanosarcina acetivorans*. J Bacteriol 188:702-710.
- 691 25. Reichlen MJ, Vepachedu VR, Murakami KS, Ferry JG. 2012. MreA functions in
692 the global regulation of methanogenic pathways in *Methanosarcina*
693 *acetivorans*. mBio 3:e00189-12.
- 694 26. Sowers KR, Boone JE, Gunsalus RP. 1993. Disaggregation of *Methanosarcina*
695 spp. and Growth as Single Cells at Elevated Osmolarity. Appl Environ
696 Microbiol 59:3832-3839.
- 697 27. Metcalf WW, Zhang JK, Shi X, Wolfe RS. 1996. Molecular, genetic, and
698 biochemical characterization of the *serC* gene of *Methanosarcina barkeri*
699 Fusaro. J Bacteriol 178:5797-5802.
- 700 28. Boccazzi P, Zhang JK, Metcalf WW. 2000. Generation of dominant selectable
701 markers for resistance to pseudomonic acid by cloning and mutagenesis of
702 the *ileS* gene from the archaeon *Methanosarcina barkeri* Fusaro. J Bacteriol
703 182:2611-2618.
- 704 29. Pritchett MA, Zhang JK, Metcalf WW. 2004. Development of a markerless
705 genetic exchange method for *Methanosarcina acetivorans* C2A and its use in
706 construction of new genetic tools for methanogenic archaea. Appl Environ
707 Microbiol 70:1425-1433.
- 708 30. Wanner BL. 1986. Novel regulatory mutants of the phosphate regulon in
709 *Escherichia coli* K-12. J Mol Biol 191:39-58.

- 710 31. Miller VL, Mekalanos JJ. 1988. A novel suicide vector and its use in
711 construction of insertion mutations: osmoregulation of outer membrane
712 proteins and virulence determinants in *Vibrio cholerae* requires *toxR*. J
713 Bacteriol 170:2575-2583.
- 714 32. Ausubel FM, Brent R, Kingston RE, Moore DD, Seidman JG, Smith JA, Struhl K.
715 1992. Current Protocols in Molecular Biology. Wiley & Sons, New York.
- 716 33. Metcalf WW, Zhang JK, Apolinario E, Sowers KR, Wolfe RS. 1997. A genetic
717 system for Archaea of the genus *Methanosarcina*: liposome-mediated
718 transformation and construction of shuttle vectors. Proc Natl Acad Sci U S A
719 94:2626-2631.
- 720 34. Zhang JK, White AK, Kuettner HC, Boccazzi P, Metcalf WW. 2002. Directed
721 mutagenesis and plasmid-based complementation in the methanogenic
722 archaeon *Methanosarcina acetivorans* C2A demonstrated by genetic analysis
723 of proline biosynthesis. J Bacteriol 184:1449-1454.
- 724 35. Bradford MM. 1976. A rapid and sensitive method for the quantitation of
725 microgram quantities of protein utilizing the principle of protein-dye binding.
726 Anal Biochem 72:248-254.
- 727 36. Stewart FJ, Ottesen EA, DeLong EF. 2010. Development and quantitative
728 analyses of a universal rRNA-subtraction protocol for microbial
729 metatranscriptomics. ISME J 4:896-907.
- 730 37. Fu H, Metcalf WW. 2015. Genetic basis for metabolism of methylated sulfur
731 compounds in *Methanosarcina* species. J Bacteriol 197:1515-1524.

732 38. Robinson MD, Smyth GK. 2008. Small-sample estimation of negative binomial
733 dispersion, with applications to SAGE data. *Biostatistics* 9:321-332.

734

735

736 **FIGURE LEGENDS**

737 **Fig 1. Hydrogenase operons of *Methanosarcina barkeri*.** Three distinct types of
738 hydrogenase are encoded by *M. barkeri*. Two potential methanophenazine-
739 dependent hydrogenases are encoded by the adjacent *vhtGACD* and *vhxGAC* operons,
740 while two potential F420-dependent hydrogenases are encoded by the unlinked
741 *frhADGB* and *freAEGB* operons. The energy-converting, ferredoxin-dependent
742 hydrogenase is encoded by the *echABCDEFGH* operon. Locus Tags are shown below
743 each gene, in some cases the “Mbar_” prefix was omitted (shown by an asterisk) due
744 to space constraints.

745

746 **Fig 2. Four methanogenic pathways of *Methanosarcina*.** Each pathway shares a
747 common step in the reduction of methyl-CoM to methane; however, they differ in
748 the route used to form methyl-CoM and in the source of electrons used for its
749 reduction to methane. The CO₂ reduction pathway (red arrows) involves reduction
750 of CO₂ to methane using electrons derived from the oxidation of H₂, while the
751 methylotrophic pathway (light blue arrows) involves disproportionation of C-1
752 substrates to methane and CO₂. These two pathways share many steps, with overall
753 metabolic flux in opposite directions (shown by red/light blue shaded arrows). In
754 the acetoclastic pathway (green arrows), acetate is split into a methyl group and an
755 enzyme-bound carbonyl moiety (shown in brackets) by the enzyme acetyl-CoA
756 decarbonylase/synthase (ACDS). The latter is oxidized to CO₂, producing reduced
757 ferredoxin that provides electrons for reduction of methyl group to methane. Lastly,
758 in the methyl reduction pathway (dark blue arrows) C-1 compounds are reduced to

759 CH₄ using electrons derived from H₂ oxidation. Dashed lines depict diffusion of H₂,
760 which occurs during the transfer of electrons between oxidative and reductive
761 portions of methylotrophic and acetoclastic pathways. The steps catalyzed by Frh,
762 Vht, Ech hydrogenases are indicated. Note that in wild-type *M. barkeri* hydrogenases
763 are involved in all four pathways. Abbreviations used are: Hdr, heterodisulfide
764 reductase; MF, methanofuran; H₄SPT, tetrahydrosarcinapterin; CoM, coenzyme M;
765 CoB, coenzyme B; CoM-S-S-CoB, heterodisulfide of CoM and CoB; Fd_{ox}/Fd_{red},
766 oxidized and reduced ferredoxin; F420_{ox}/F420_{red}, oxidized and reduced cofactor
767 F420; MP_{ox}/MP_{red}, oxidized and reduced methanophenazine.

768

769 **Fig 3. The branched electron transport systems of *Methanosarcina barkeri* and**
770 ***Methanosarcina acetivorans*.** During methylotrophic methanogenesis, *M. barkeri*
771 can utilize H₂-dependent or H₂-independent electron transport systems. The H₂-
772 dependent pathway involves the use of hydrogenases Frh, Ech, and Vht in a H₂
773 cycling mechanism to transfer electrons from F420_{red} or Fd_{red} to methanophenazine
774 (MP). *M. acetivorans* does not utilize hydrogenases, and is therefore incapable of H₂
775 cycling. Both organisms can conserve energy via a H₂-independent pathway,
776 wherein electrons are transferred from F420_{red} to MP by way of the F420
777 dehydrogenase (Fpo). Additionally, the electron transport system in *M. acetivorans*
778 includes the Na⁺-translocating Rnf enzyme complex that serves as a Fd:MP
779 oxidoreductase. Both membrane-bound electron transport systems converge at the
780 reduction of the CoM-S-S-CoB heterodisulfide with electrons from reduced MP_{red} via
781 the cytochrome-containing HdrDE enzyme. Protons (or Na⁺ in the case of Rnf) are

782 translocated across the cell membrane in both systems, thereby conserving energy
783 in the form of an ion motive force. An additional heterodisulfide reductase,
784 HdrA1B1C1, has been proposed to function in the energy conservation pathways for
785 both organisms. This electron bifurcating enzyme potentially reduces both the CoM-
786 S-S-CoB heterodisulfide and F420 with electrons from Fd_{red} at a stoichiometric ratio
787 of 2 Fd_{red} oxidized for the reduction of 1 CoM-S-S-CoB to CoM-SH/CoB-SH and
788 reduction of 1 F420_{ox} to F420_{red}. Abbreviations used are: Fd_{ox}/Fd_{red}, oxidized and
789 reduced ferredoxin; MP/MPH₂, oxidized and reduced methanophenazine;
790 F420_{ox}/F420_{red}, oxidized and reduced F420; CoM, coenzyme M; CoB, coenzyme B;
791 CoM-S-S-CoB, heterodisulfide of CoM and CoB; FeS, iron-sulfur cluster; FAD, flavin
792 adenine dinucleotide; FMN, flavin mononucleotide; NiFe, nickel-iron active site of
793 hydrogenases; cytb₁/cytb₂/cyt c, cytochromes.
794

795 TABLES

796 Table 1. Growth of *M. barkeri* mutant strains on various methanogenic substrates.

Genotype	H ₂ /CO ₂			Methanol			Methanol/H ₂ /CO ₂			Acetate		
	Gen. (h) ^d	Max. OD ^e	Lag (h)	Gen. (h) ^d	Max. OD ^e	Lag (h)	Gen. (h) ^d	Max. OD ^e	Lag (h)	Gen. (h) ^d	Max. OD ^f	Lag (h)
<i>Δhpt</i> ^a	10.4 ± 0.7	0.42 ± 0.04	49 ± 11	8.9 ± 0.3	0.85 ± 0.05	36 ± 1	6.2 ± 0.5	0.77 ± 0.03	33 ± 1	43.6 ± 2.2	1.65 ± 0.04	195 ± 11
<i>Δfre</i>	10.3 ± 0.6	0.35 ± 0.03	59 ± 1	8.8 ± 0.4	0.78 ± 0.04	37 ± 1	7.0 ± 0.4	0.68 ± 0.01	38 ± 4	38.6 ± 2.3	1.68 ± 0.05	200 ± 13
<i>Δvhx</i>	10.7 ± 0.5	0.45 ± 0.02	60 ± 3	8.5 ± 0.2	0.78 ± 0.08	36 ± 2	7.5 ± 0.5	0.69 ± 0.04	51 ± 3	47.2 ± 3.8	1.70 ± 0.08	181 ± 22
<i>Δech</i>	NG	NA	NA	12.2 ± 0.9	0.69 ± 0.05	46 ± 1	NG	NA	NA	NG	NA	NA
<i>Δech/Δfrh</i>	NG	NA	NA	12.1 ± 0.7	0.80 ± 0.05	54 ± 2	13 ± 2	0.54 ± 0.03	248 ± 17	NG	NA	NA
<i>Δech/Δfrh/Δvht</i>	NG	NA	NA	10.8 ± 0.2	0.71 ± 0.06	48 ± 3	9.0 ± 0.4	0.61 ± 0.02	48 ± 2	NG	NA	NA
<i>Δech/Δfrh/Δfre/Δvht-vhx</i> ^c	NG	NA	NA	12.1 ± 0.2	0.84 ± 0.06	54 ± 2	9.3 ± 0.1	0.68 ± 0.03	45 ± 1	NG	NA	NA
<i>P_{tet}vht</i> ^b	NG	NA	NA	NG	NA	NA	NG	NA	NA	NG	NA	NA
<i>P_{tet}vht/Δech</i> ^b	NG	NA	NA	NG	NA	NA	NG	NA	NA	NG	NA	NA
<i>Δfrh/Δvht</i>	NG	NA	NA	11.7 ± 0.7	0.89 ± 0.01	54 ± 2	35 ± 3	0.33 ± 0.03	151 ± 4	NG	NA	NA
<i>Δfrh/Δfre/Δvht-vhx</i> ^c	NG	NA	NA	12.3 ± 0.6	0.84 ± 0.07	58 ± 2	29 ± 2	0.43 ± 0.03	116 ± 3	NG	NA	NA
<i>Δfrh</i>	NG	NA	NA	19.5 ± 1.0	0.69 ± 0.05	122 ± 6	7.4 ± 0.6	0.64 ± 0.14	45 ± 3	38.2 ± 1.7	1.71 ± 0.03	219 ± 11
<i>Δfrh/Δfre</i>	NG	NA	NA	16.5 ± 0.8	0.80 ± 0.00	89 ± 2	7.7 ± 0.2	0.74 ± 0.01	48 ± 1	39.6 ± 2.9	1.63 ± 0.07	170 ± 13

797

798 ^a *M. barkeri* Fusaro parental strain; ^b Growth in the absence of tetracycline; ^c *Mbar_A1842* and *Mbar_1843* also deleted; ^d
799 Generation (doubling) time; ^e Optical Density was measured on a Spectronic 20 spectrophotometer at 600 nm; ^f Optical
800 Density was measured on a Hewlett Packard 8453 spectrophotometer at 600 nm. Note that an OD of 1.0 on the Hewlett
801 Packard 8453 is equivalent to an OD of ~0.2 on the Spectronic 20. NG, no growth for at least 6 months of incubation; NA, not
802 applicable.

803 **Table 2. Production of CH₄ and CO₂ from resting cell suspensions of *M. barkeri* mutant strains.**

Genotype	H ₂ /CO ₂		Methanol			Methanol/H ₂		
	CH ₄ ^a	CO ₂ ^a	CH ₄ ^a	CO ₂ ^a	CH ₄ : CO ₂	CH ₄ ^a	CO ₂ ^a	CH ₄ : CO ₂
<i>Δhpt</i> ^b	307 ± 24	NA	339 ± 6	118 ± 2	2.9:1	458 ± 6	< 1	
<i>Δfre</i>	316 ± 16	NA	339 ± 7	117 ± 2	2.9:1	442 ± 24	< 1	
<i>Δvhx</i>	328 ± 21	NA	329 ± 7	113 ± 3	2.9:1	453 ± 6	< 1	
<i>Δech</i>	5 ± 1	NA	331 ± 6	109 ± 2	3.0:1	460 ± 12	< 1	
<i>Δech/Δfrh</i>	3 ± 0	NA	328 ± 7	107 ± 2	3.1:1	440 ± 14	4 ± 1	110:1
<i>Δech/Δfrh/Δvht</i>	1 ± 0	NA	315 ± 5	93 ± 1	3.4:1	313 ± 5	92 ± 2	3.4:1
<i>Δech/Δfrh/Δfre/Δvht-vhx</i> ^c	1 ± 0	NA	314 ± 2	94 ± 1	3.3:1	315 ± 8	93 ± 3	3.4:1
<i>Δfrh</i>	34 ± 1	NA	310 ± 8	96 ± 2	3.2:1	442 ± 4	< 1	
<i>Δfrh/Δfre</i>	10 ± 2	NA	298 ± 13	98 ± 4	3.0:1	436 ± 8	< 1	
<i>Δfrh/Δvht</i>	6 ± 1	NA	311 ± 5	92 ± 1	3.4:1	225 ± 16	20 ± 1	11:1
<i>Δfrh/Δfre/Δvht-vhx</i> ^c	5 ± 0	NA	309 ± 6	92 ± 2	3.4:1	300 ± 8	19 ± 1	16:1

804 ^a μmol product observed; ^b *M. barkeri* Fusaro parental strain; ^c *Mbar_A1842* and *Mbar_1843* also deleted; NA, not applicable as
805 produced CO_2 could not be differentiated from CO_2 that was added to the headspace. When relevant, ratio of $\text{CH}_4:\text{CO}_2$ is shown.
806 CH_4 and CO_2 quantities were below $4 \pm 1 \mu\text{mol}$ for each strain when measured in cell suspensions without substrate.

807 **Table 3. Rate of CH₄ production^a from resting cell suspensions of *M. barkeri***
808 **mutant strains.**

Genotype	Methanol	Methanol & H ₂
Δhpt^b	86 ± 7	132 ± 18
Δfre	84 ± 1	123 ± 16
Δvhx	71 ± 2	74 ± 12
Δech	57 ± 5	122 ± 7
$\Delta ech/\Delta frh$	20 ± 1	27 ± 3
$\Delta ech/\Delta frh/\Delta vht$	31 ± 2	30 ± 3
$\Delta ech/\Delta frh/\Delta fre/\Delta vht-vhx^c$	19 ± 2	19 ± 2
Δfrh	23 ± 1	136 ± 9
$\Delta frh/\Delta fre$	14 ± 1	87 ± 3
$\Delta frh/\Delta vht$	38 ± 8	36 ± 4
$\Delta frh/\Delta fre/\Delta vht-vhx^c$	32 ± 10	34 ± 13

809 ^a nmol methane produced min⁻¹ mg⁻¹; ^b *M. barkeri* Fusaro parental strain; ^c

810 *Mbar_A1842* and *Mbar_1843* also deleted.

811

812

813 **Table 4. Hydrogenase activity of *M. barkeri* mutant strains.**

Genotype	Specific Activity ^a
Δhpt^b	11.10 ± 4.29
Δfre	9.18 ± 4.38
Δvhx	8.51 ± 3.93
$\Delta ech/\Delta frh/\Delta vht$	0.01 ± 0.00^d
$\Delta ech/\Delta frh/\Delta fre/\Delta vht-vhx^c$	0.02 ± 0.00
Δech	17.13 ± 4.90
$\Delta frh/\Delta vht$	0.42 ± 0.09
$\Delta ech/\Delta frh$	2.60 ± 1.36
Δfrh	3.12 ± 1.89

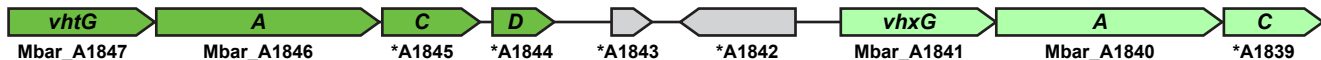
814 ^aμmol H₂ oxidized min⁻¹ mg⁻¹; ^b *M. barkeri* Fusaro parental strain; ^c *Mbar_A1842* and

815 *Mbar_A1843* also deleted; ^d values that are significantly different (p-value < 0.01)

816 than the Δhpt parental strain are indicated in bold.

817

Methanophenazine-reducing hydrogenase operons



Ferredoxin-reducing hydrogenase operon



F420-reducing hydrogenase operons

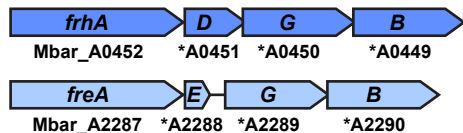


Fig 1. Hydrogenase operons of *Methanosarcina barkeri*. Three distinct types of hydrogenase are encoded by *M. barkeri*. Two potential methanophenazine-dependent hydrogenases are encoded by the adjacent *vhtGACD* and *vhxGAC* operons, while two potential F420-dependent hydrogenases are encoded by the unlinked *frhADGB* and *freAEGB* operons. The energy-converting, ferredoxin-dependent hydrogenase is encoded by the *echABCDEF* operon. Locus Tags are shown below each gene, in some cases the “Mbar_” prefix was omitted (shown by an asterisk) due to space constraints.

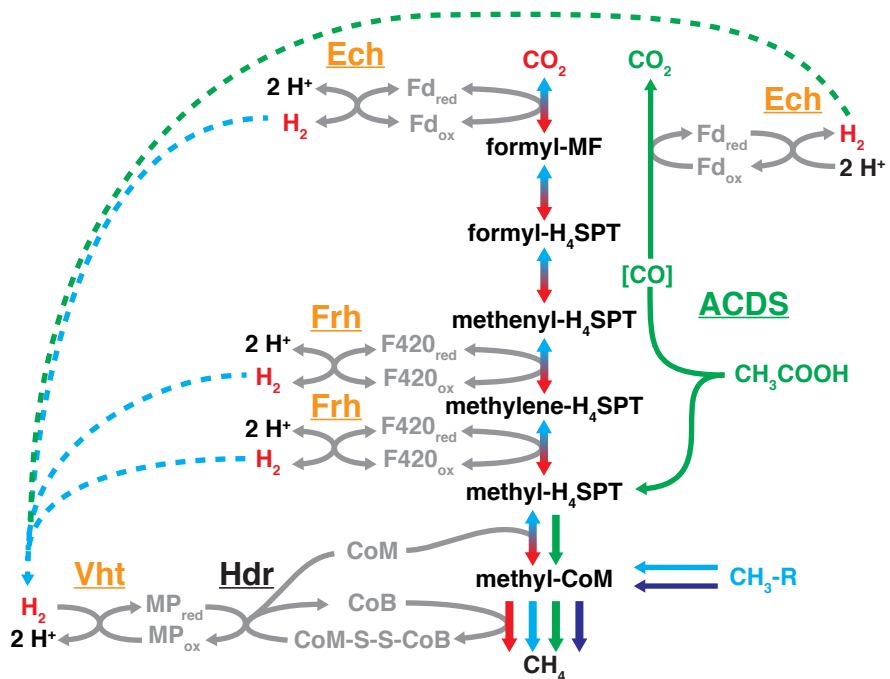
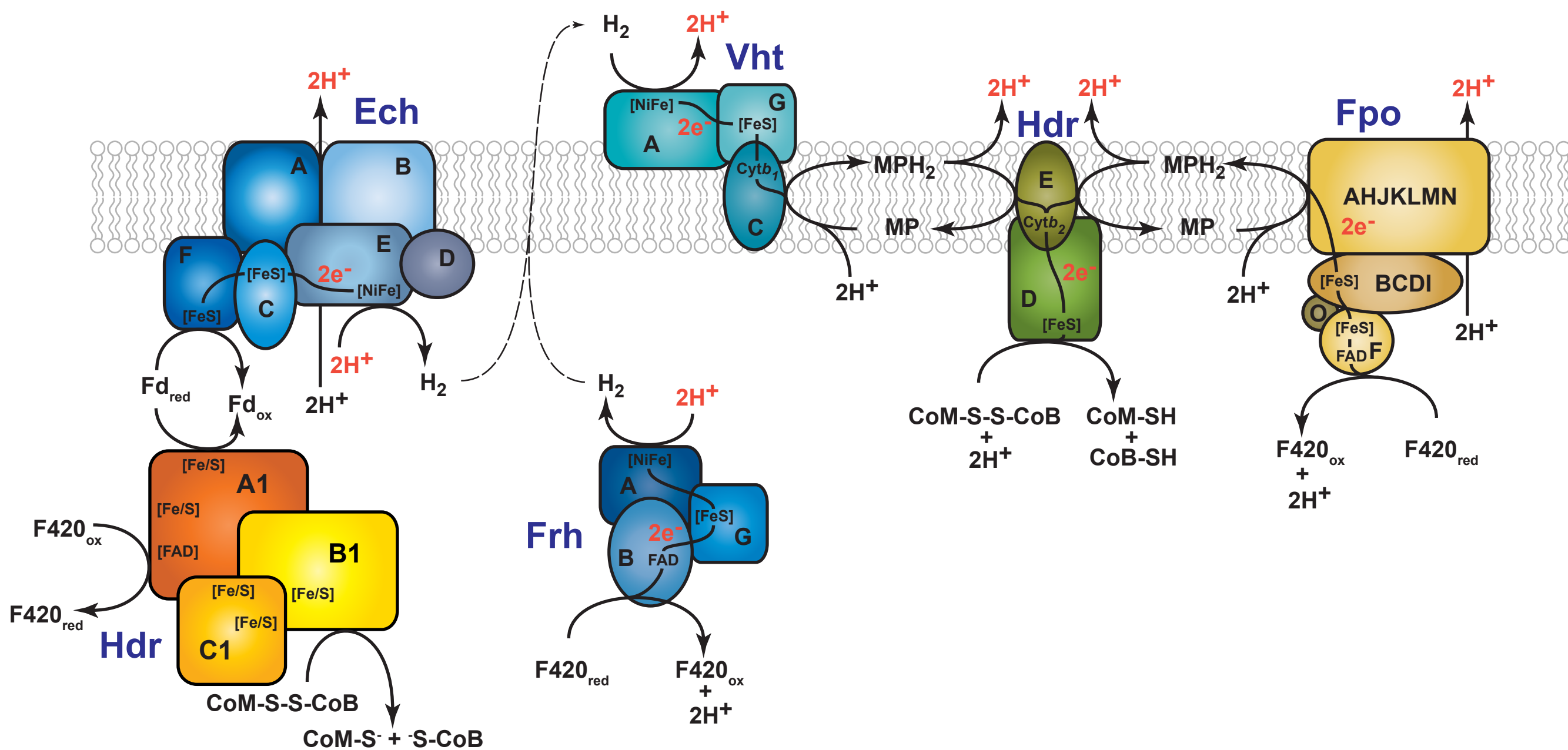


Fig 2. Four methanogenic pathways of *Methanosarcina*. Each pathway shares a common step in the reduction of methyl-CoM to methane; however, they differ in the route used to form methyl-CoM and in the source of electrons used for its reduction to methane. The CO₂ reduction pathway (red arrows) involves reduction of CO₂ to methane using electrons derived from the oxidation of H₂, while the methylotrophic pathway (light blue arrows) involves disproportionation of C-1 substrates to methane and CO₂. These two pathways share many steps, with overall metabolic flux in opposite directions (shown by red/light blue shaded arrows). In the aceticlastic pathway (green arrows), acetate is split into a methyl group and an enzyme-bound carbonyl moiety (shown in brackets) by the enzyme acetyl-CoA decarbonylase/synthase (ACDS). The latter is oxidized to CO₂, producing reduced ferredoxin that provides electrons for reduction of methyl group to methane. Lastly, in the methyl reduction pathway (dark blue arrows) C-1 compounds are reduced to CH₄ using electrons derived from H₂ oxidation. Dashed lines depict diffusion of H₂, which occurs during the transfer of electrons between oxidative and reductive portions of methylotrophic and aceticlastic pathways. The steps catalyzed by Frh, Vht, Ech hydrogenases are indicated. Note that in wild-type *M. barkeri* hydrogenases are involved in all four pathways. Abbreviations used are: Hdr, heterodisulfide reductase; MF, methanofuran; H₄SPT, tetrahydrosarcinapterin; CoM, coenzyme M; CoB, coenzyme B; CoM-S-S-CoB, heterodisulfide of CoM and CoB; Fd_{ox}/F_d_{red}, oxidized and reduced ferredoxin; F420_{ox}/F420_{red}, oxidized and reduced cofactor F420; MP_{ox}/MP_{red}, oxidized and reduced methanophenazine.

Methanosarcina barkeri



bioRxiv preprint doi: <https://doi.org/10.1101/334656>; this version posted May 20, 2018. The copyright holder for this preprint (which was not certified by peer review) is the author/funder. All rights reserved. No reuse allowed without permission.

Methanosarcina acetivorans

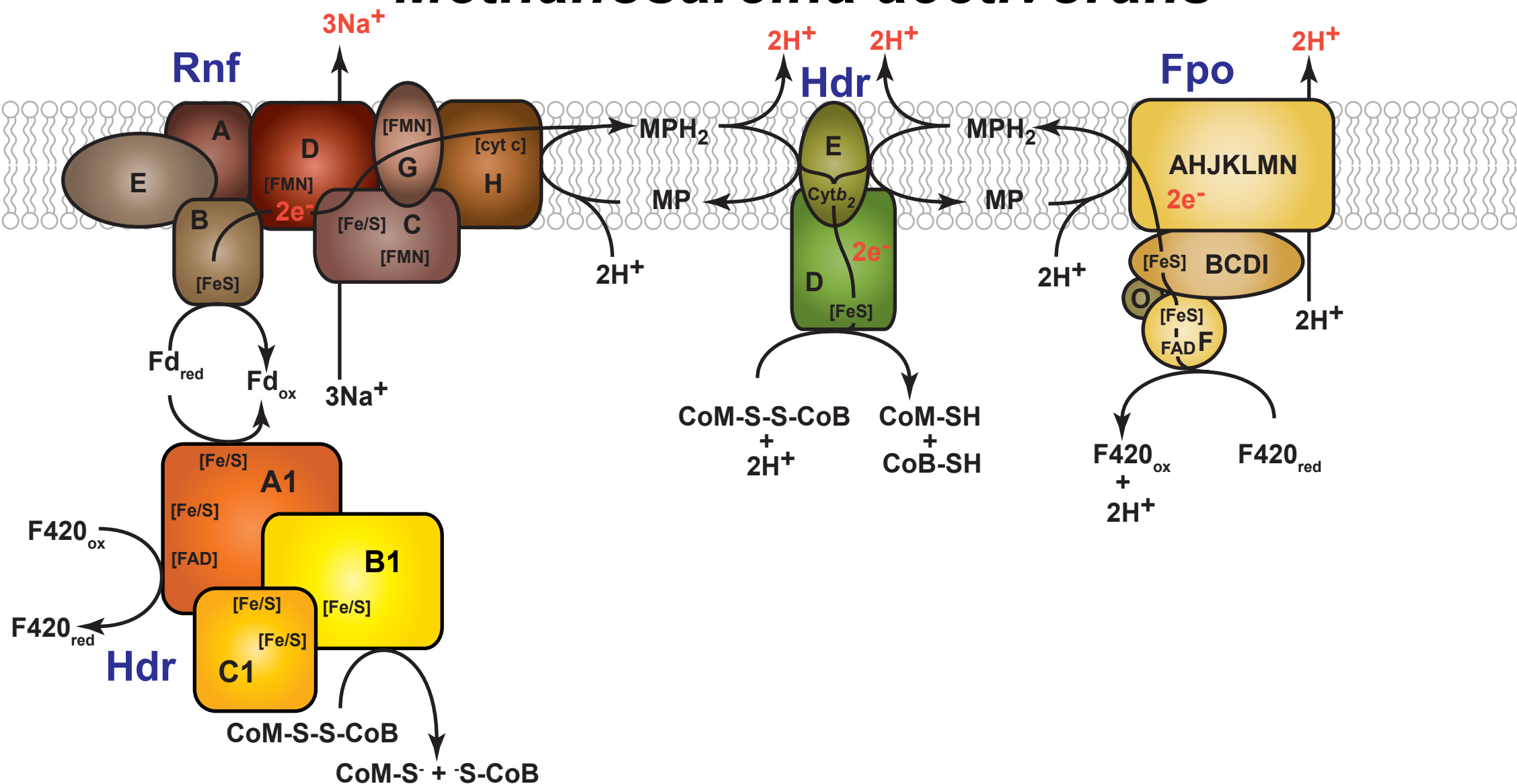


Fig 3. The branched electron transport systems of *Methanosarcina barkeri* and *Methanosarcina acetivorans*. During methylotrophic methanogenesis, *M. barkeri* can utilize H₂-dependent or H₂-independent electron transport systems. The H₂-dependent pathway involves the use of hydrogenases Frh, Ech, and Vht in a H₂ cycling mechanism to transfer electrons from F420_{red} or Fd_{red} to methanophenazine (MP). *M. acetivorans* does not utilize hydrogenases, and is therefore incapable of H₂ cycling. Both organisms can conserve energy via a H₂-independent pathway, wherein electrons are transferred from F420_{red} to MP by way of the F420 dehydrogenase (Fpo). Additionally, the electron transport system in *M. acetivorans* includes the Na⁺-translocating Rnf enzyme complex that serves as a Fd:MP oxidoreductase. Both membrane-bound electron transport systems converge at the reduction of the CoM-S-S-CoB heterodisulfide with electrons from reduced MP_{red} via the cytochrome-containing HdrDE enzyme. Protons (or Na⁺ in the case of Rnf) are translocated across the cell membrane in both systems, thereby conserving energy in the form of an ion motive force. An additional heterodisulfide reductase, HdrA1B1C1, has been proposed to function in the energy conservation pathways for both organisms. This electron bifurcating enzyme potentially reduces both the CoM-S-S-CoB heterodisulfide and F420 with electrons from Fd_{red} at a stoichiometric ratio of 2 Fd_{red} oxidized for the reduction of 1 CoM-S-S-CoB to CoM-SH/CoB-SH and reduction of 1 F420_{ox} to F420_{red}. Abbreviations used are: Fd_{ox}/Fd_{red}, oxidized and reduced ferredoxin; MP/MPH₂, oxidized and reduced methanophenazine; F420_{ox}/F420_{red}, oxidized and reduced F420; CoM, coenzyme M; CoB, coenzyme B; CoM-S-S-CoB, heterodisulfide of CoM and CoB; FeS, iron-sulfur cluster; FAD, flavin adenine dinucleotide; FMN, flavin mononucleotide; NiFe, nickel-iron active site of hydrogenases; cytb1/cytb2/cyt c, cytochromes.